

# PROCEEDINGS OF SPIE

[SPIDigitalLibrary.org/conference-proceedings-of-spie](https://spiedigitallibrary.org/conference-proceedings-of-spie)

## Estimation of surface spectral reflectance of inhomogeneous objects

Shoji Tominaga, Brian A. Wandell

Shoji Tominaga, Brian A. Wandell, "Estimation of surface spectral reflectance of inhomogeneous objects," Proc. SPIE 1260, Sensing and Reconstruction of Three-Dimensional Objects and Scenes, (1 January 1990); doi: 10.1117/12.20009

**SPIE.**

Event: Electronic Imaging: Advanced Devices and Systems, 1990, Santa Clara, CA, United States

# Estimation of Surface Spectral Reflectance of Inhomogeneous Objects

Shoji Tominaga

Faculty of Engineering, Osaka Electro-Communication University, Neyagawa, Osaka 572, Japan  
and

Brian A. Wandell

Department of Psychology, Stanford University, Stanford, California 94305, USA

## Abstract

This paper describes a method for estimating the surface spectral reflectance function of inhomogeneous objects. The standard reflectance model for inhomogeneous materials suggests that surface reflectance functions can be described as the sum of a constant (specular) function and a subsurface (diffuse) function. First we present an algorithm to generate an illuminant estimate without using a reference white standard. Next we show that several physical constraints on the reflectance functions can be used to estimate the subsurface component. A band of the estimated spectral reflectance functions is recovered as possible solutions for the subsurface component.

## 1 Introduction

The visual information that we use to perceive an object in a scene is derived from the light reflected from the object and the light reflected from nearby objects. The spectral composition of the reflected light depends on the surface-reflectance properties of the objects and the spectral composition of the ambient lighting. An object's color appearance often is predicted more closely by the object's surface reflectance than by the spectral composition of the light reflected from the object. The human ability to discount the effect of some changes in the ambient lighting is called color constancy. This fact has motivated the construction of algorithms to recover object surface-reflectance functions from the observations of the reflected light<sup>1</sup>. The surface reflectance function is characteristic of an object surface. This function is inherent to the surface, and independent of variable lighting conditions. Therefore it becomes an important clue for object perception in computer vision. Accurate modeling of surface-reflectance functions also has become important in the field of computer graphics, where knowledge of surface-reflectance properties permits more accurate rendering of object appearance<sup>2</sup>.

Inhomogeneous objects are substances composed of different component materials, such as a vehicle at the surface layer and embedded pigments at the colorant layer. For example, plastics and paints are inhomogeneous. The skins of natural products like apples are also regarded to be inhomogeneous. On the other hand, typical examples of homogeneous objects are metals and crystals. For homogeneous materials, the incident light suffers no scattering; the light is reflected in accordance with Fresnel's law. Homogeneous objects are not represented by a simple reflectance model. The standard reflectance model for inhomogeneous materials suggests that, under all viewing geometries, surface reflectance functions can be described as the weighted sum of two functions<sup>3,4</sup>. One function represents the interface (specular) reflection, and the second function represents the subsurface (diffuse) reflection. From the point of view of surface identification, the subsurface reflectance function is characteristic of the surface and therefore an important clue

as to the surface's identity. The interface term is not very informative about the surface's identity.

In this paper we describe a method for estimating the subsurface component of the surface reflectance function for inhomogeneous objects. We have shown that if the standard reflectance model is correct, and further the spectral composition of the specular component is the same as the spectral composition of the incident light, then estimating the illuminant spectrum can be reduced to finding the common spectral information from the measurements from two or more surfaces<sup>4</sup>. We first summarize an algorithm to generate an illuminant estimate without using a reference white standard.

By the knowledge of an illuminant spectrum, we can define a two-dimensional space of surface reflectances. The second step toward reflectance estimation is to determine the subsurface component of the two-dimensional reflectance function. We show that several physical constraints on the surface reflectance function can be used for estimating the subsurface component. A solution method, that we call the quarter circle analysis, is introduced. The feasibility of our estimation method is evaluated on experiments.

## 2 Standard reflectance model

Light reflected from an object surface can be decomposed into two additive components, the interface reflection and the subsurface reflection (see Fig. 1). The radiance of the reflected light  $Y(\theta, \lambda)$  is a function of the wavelength  $\lambda$ , ranging over a visible wavelength, and the parameters  $\theta$ , including the direction angles of a reflectance geometry such as the incident angle, the viewing angle, and the phase angle. The standard reflectance model assumes that the color signal  $Y(\theta, \lambda)$  can be expressed as a linear combination of the two component vectors of light reflection

$$Y(\theta, \lambda) = c_I(\theta)L_I(\lambda) + c_S(\theta)L_S(\lambda), \quad (1)$$

where the terms  $L_I(\lambda)$  and  $L_S(\lambda)$  are the spectral power distributions of the interface and subsurface reflection components, respectively. The weighting terms  $c_I(\theta)$  and  $c_S(\theta)$  are the geometric scale factors. It should be noted that the spectral composition of each of the reflection components is unchanged as the viewing angle varies. The two vectors  $L_I(\lambda)$  and  $L_S(\lambda)$  span a two-dimensional space of the possible observations. All the color signals observed from an inhomogeneous surface fall in this two-dimensional subspace. We call this plane the color-signal plane P.

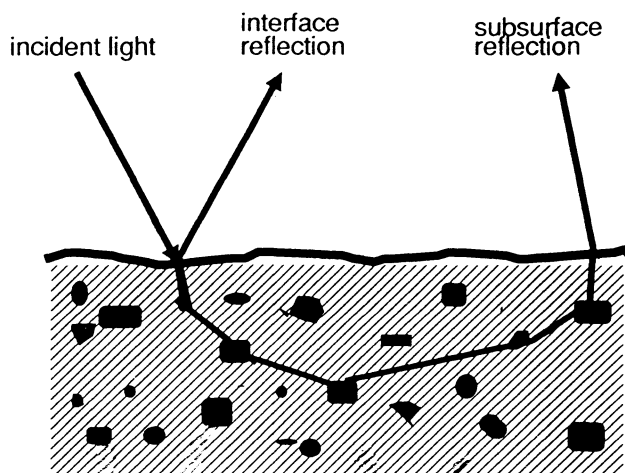


Fig. 1. Light reflection from a surface.

As we estimate the surface-reflectance functions from the color signal  $Y$ , we must express the reflection model in terms of the surface reflectance of an object and the spectral power distribution of an incident light. Let  $S_I(\lambda)$  and  $S_S(\lambda)$  be the surface spectral reflectances for the two components of interface and subsurface reflections, and let  $E(\lambda)$  be the spectral power distribution of the incident light. Then reflected light is described as

$$Y(\theta, \lambda) = c_I(\theta)S_I(\lambda)E(\lambda) + c_S(\theta)S_S(\lambda)E(\lambda), \quad (2)$$

The interface component of reflectance  $S_I(\lambda)$  is determined by Fresnel's law. If the refractive index at the surface is constant over the visible wavelength, then the interface component is independent of wavelength. A satisfactory assumption for inhomogeneous materials is as follows. The interface component of surface spectral reflectance is constant over the visible wavelength as  $S_I(\lambda) = \text{constant}$ .

### 3 Illuminant estimation

#### A. Principle

The assumption of constant specular reflectance leads to an important practical consequence that the color-signal information from inhomogeneous objects can be used to estimate the spectral power distribution of the illuminant. Suppose that we measure color signals reflected from two surfaces of inhomogeneous material under the same light source. When we measure the reflected lights with different geometric conditions, then the data form two different color-signal planes  $P(1)$  and  $P(2)$  in the space. By the assumption of constant specular reflection, the spectral power distributions of color signals for the two surfaces can be described as follows:

$$Y_1(\theta, \lambda) = c_{I_1}(\theta)E(\lambda) + c_{S_1}(\theta)S_{S_1}(\lambda)E(\lambda), \quad (3)$$

$$Y_2(\theta, \lambda) = c_{I_2}(\theta)E(\lambda) + c_{S_2}(\theta)S_{S_2}(\lambda)E(\lambda), \quad (4)$$

The planes  $P(i)(i = 1, 2)$  are constructed by a set of two vectors  $[E(\lambda), S_{S_i}(\lambda)E(\lambda)]$ . Note that the illuminant vector  $E(\lambda)$  is contained in both planes. This vector represents the common spectral information that is due to the light source. The two planes must intersect at this vector, as shown in Fig. 2. Thus we conclude that two color-signal planes from inhomogeneous objects under the same illuminant must intersect. The vector of their intersection must be in the direction of the illuminant vector. Therefore the estimation problem of an illuminant spectrum is reduced to a computational problem of finding an intersection of two color-signal planes. This property can be extended to many surfaces.

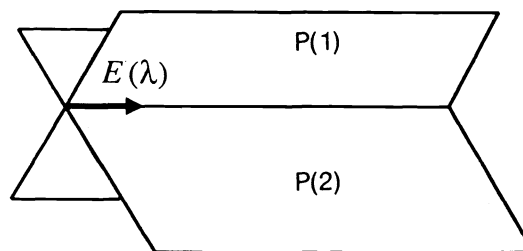


Fig. 2. Intersection of two color-signal planes.

#### B. Computation

Let us assume that we observe  $m$  color signals reflected from an object surface under various geometric conditions but with a constant illuminant. We sample each spectral power distribution at  $n$  points of  $\lambda$ . The  $m$  color signals are represented by  $n$ -dimensional column vectors denoted by  $\mathbf{y}_i$  ( $i = 1, 2, \dots, m$ ). If

a set of data vectors falls in a subspace, their normalized representations fall in the same plane. So we perform all our calculations by using the normalized spectral power distributions as  $\| \mathbf{y}_i \|^2 = 1$ . All the normalized spectral power distributions are summarized in an  $n \times m$  matrix  $\mathbf{Y}$  ( $= [\mathbf{y}_1, \mathbf{y}_2, \dots, \mathbf{y}_m]$ ). We use the singular-value decomposition (SVD) to determine a color signal plane from the observed light spectra. The measured color signals then fall into a two-dimensional subspace of the  $n$ -dimensional vector space  $\mathbf{R}^n$  when the rank of  $\mathbf{Y}$  is 2. Let  $\mathbf{u}_1$  and  $\mathbf{u}_2$  be the first two vectors of the  $n$ -dimensional left-hand singular vectors in the SVD of  $\mathbf{Y}$ . These vectors are a set of basis vectors that span a two-dimensional subspace of  $\mathbf{R}^n$ . Therefore the color-signal plane of the object surface can be determined as

$$P = \{ \mathbf{y} \mid \mathbf{y} = c_1 \mathbf{u}_1 + c_2 \mathbf{u}_2, \quad c_i \in R \}. \quad (5)$$

The set  $R$  is a set of real numbers such that  $\mathbf{y}$  is nonnegative and physically realizable.

Next let us assume that two object surfaces are observed under the same light source. Two color-signal planes are determined from the SVD's of the two data sets. Let  $[\mathbf{u}_1(1), \mathbf{u}_2(1)]$  and  $[\mathbf{u}_1(2), \mathbf{u}_2(2)]$  be the basis vectors of the color-signal planes  $P(1)$  and  $P(2)$ . Since the intersection line must lie in both  $P(1)$  and  $P(2)$ , we have the relation

$$c_1 \mathbf{u}_1(1) + c_2 \mathbf{u}_2(1) = c'_1 \mathbf{u}_1(2) + c'_2 \mathbf{u}_2(2). \quad (6)$$

A nontrivial solution of this equation defines the intersection of the planes. The details of a solution method are given in Ref.4 to obtain an estimate  $\mathbf{e}$  for  $E(\lambda)$ .

## 4 Recovering surface spectral reflectance

### 4.1 Physical constraints

Using our estimate of the ambient light, we can define the two-dimensional space of surface reflectances by dividing the two-dimensional space of color signals by  $E(\lambda)$ .

$$\frac{Y(\theta, \lambda)}{E(\lambda)} = S(\theta, \lambda) = c_I(\theta) S_I(\lambda) + c_S(\theta) S_S(\lambda). \quad (7)$$

Note that this surface reflectance plane defined by  $S_I(\lambda)$  and  $S_S(\lambda)$  does not change with different illuminants. The surface reflectance plane is inherent to the object surface, unlike the color signal plane defined by  $L_I(\lambda)$  and  $L_S(\lambda)$ . By hypothesis, the interface component  $S_I(\lambda)$  of the two dimensions is a constant specular function. The subsurface function  $S_S(\lambda)$  must be

- (a) all nonnegative over the visible wavelength as  $S_S(\lambda) \geq 0$ , and
- (b) contribute only nonnegative weights for all of the measured color signals as  $c_S(\theta) \geq 0$ .

Lawton and Sylvestre<sup>5</sup> treated the general problem of determining the shapes of two functions with such physical constraints from an observed set of additive mixture of the two functions. Their method produces two bands of estimated functions. In our application, one function,  $S_I(\lambda)$ , is fixed. It should be noted that the problem is to estimate a band of the subsurface reflectance functions, rather than to estimate a unique  $S_S(\lambda)$ . That is, we can recover only a range of subsurface estimates, not a unique estimate. Here we introduce the special case of the Lawton and Sylvestre analysis that we call the quarter circle analysis.

### 4.2 Quarter circle analysis

#### A. Observation of surface reflectances

First assume that we measure  $m$  color signals from an object surface under geometric conditions  $\theta_1, \theta_2, \dots, \theta_m$ .

Each color signal  $Y(\theta_i, \lambda)$  ( $i = 1, 2, \dots, m$ ), is sampled at  $\lambda_1, \lambda_2, \dots, \lambda_n$ . Next let  $\hat{E}(\lambda_j)$  ( $j = 1, 2, \dots, n$ ) be an estimate of the spectral power distribution of the illuminant. Then the observations of  $m$  surface spectral reflectances are obtained by  $S(\theta_i, \lambda_j) = Y(\theta_i, \lambda_j)/\hat{E}(\lambda_j)$ . We represent these reflectances by  $n$ -dimensional column vectors  $\mathbf{s}_i$  ( $i = 1, 2, \dots, m$ ). These vectors are normalized so that  $\|\mathbf{s}_i\|^2 = 1$ .

Since the surface spectral reflectances are two-dimensional, the normalized reflectances  $\mathbf{s}_i$  can be represented in term of two orthonormal basis vectors as

$$\mathbf{s}_i = p_{i1}\mathbf{u}_1 + p_{i2}\mathbf{u}_2, \quad (i = 1, 2, \dots, m), \quad (8)$$

This orthogonal expansion can be determined using the SVD of an  $n$ -by- $m$  matrix of the observed reflectances. The vectors  $\mathbf{u}_1$  and  $\mathbf{u}_2$  are the first two of the  $n$ -dimensional left singular vectors. The coefficients  $p_{i1}$  and  $p_{i2}$  are specified from the singular values and the elements of the right singular vectors. We have  $\mathbf{u}_1 \geq 0$  ( $u_{j1} \geq 0, j = 1, 2, \dots, n$ ) and  $p_{i1} \geq 0$ . However because of the orthogonality, the second  $\mathbf{u}_2$  has some negative elements. Because  $\mathbf{u}_1$  is orthogonal to  $\mathbf{u}_2$ , it follows that

$$1 = \|\mathbf{s}_i\|^2 = p_{i1}^2 + p_{i2}^2. \quad (9)$$

Thus, the representation of the normalized surface reflectance measurements will have unit length in the principal component coordinate frame  $(\mathbf{u}_1, \mathbf{u}_2)$ .

### B. Basis transformation

The unit-length basis vectors  $\mathbf{u}_1$  and  $\mathbf{u}_2$  depend upon experimental factors such as the measurement angles  $\theta$  and the number of measurements. These vectors do not characterize the surface properties. Our goal is to find a method of transforming the vectors  $\mathbf{u}_1$  and  $\mathbf{u}_2$  to a new representation that estimates a range of the subsurface reflectance vector  $\mathbf{S}_S$  for  $S_S(\lambda)$ . For conceptual simplicity, we begin by transforming the data representation from the principal component coordinates  $(p_1, p_2)$  with respect to the basis functions  $\mathbf{u}_1$  and  $\mathbf{u}_2$  into a new coordinate frame with respect to the coordinate system defined by the vector  $\mathbf{S}_I$  and a unit length vector perpendicular to  $\mathbf{S}_I$  that we call  $\mathbf{S}_I^\perp$ . From our experimental measurements  $\mathbf{S}_I$  can be obtained by a linear combination of  $\mathbf{u}_1$  and  $\mathbf{u}_2$ . Then we can find the unique unitary transformation  $\mathbf{T}$  such that

$$[\mathbf{S}_I, \mathbf{S}_I^\perp] = [\mathbf{u}_1, \mathbf{u}_2]\mathbf{T}, \quad (10)$$

The unitary transformation  $\mathbf{T}$  rotates  $\mathbf{u}_1$  into  $\mathbf{S}_I$ . The second vector  $\mathbf{S}_I^\perp$  is the unique unit-length vector that is orthogonal to  $\mathbf{S}_I$  within the surface reflectance plane.

In practice, due to measurement error and small failures of the model, the interface reflectance component  $\mathbf{S}_I$  cannot be assumed to be precisely in the plane of the first two principal components  $(\mathbf{u}_1, \mathbf{u}_2)$  of pixel data. The interface component is then obtained as the projection of a unit vector onto the  $(\mathbf{u}_1, \mathbf{u}_2)$ . The unitary matrix  $\mathbf{T}$  can be found by solving the least square problem which minimizes  $\|\mathbf{i} - t_1\mathbf{u}_1 - t_2\mathbf{u}_2\|^2$ , where  $\mathbf{i}$  is a unit vector with entries of  $1/\sqrt{n}$ . By convention we choose  $\mathbf{u}_2$  so that  $t_2$  is positive. The matrix  $\mathbf{T}$  is

$$\mathbf{T} = \frac{1}{(t_1^2 + t_2^2)^{1/2}} \begin{bmatrix} t_1 & t_2 \\ t_2 & -t_1 \end{bmatrix}. \quad (11)$$

An observation that is represented by  $(p_{i1}, p_{i2})$  in the principal component coordinate frame will be represented by  $[c_{Ii}, c_{Ii}^\perp] = [p_{i1}, p_{i2}]\mathbf{T}$  in the transformed coordinate frame.

There are several simplifying features of this coordinate frame that are illustrated in Figure 3. First, because the surface reflectances observed have been normalized to unit length, and  $\mathbf{T}$  is a unitary transformation, the coordinates  $(c_I, c_I^\perp)$  satisfy  $c_{Ii}^2 + c_{Ii}^{\perp 2} = 1$ . Thus the representation of the measurements will fall

on the unit circle. Next, the value of  $c_I$  must exceed 0 because this component describes the contribution from the interface reflectance, which is always nonnegative. Furthermore, the value of  $c_I^\perp$  is proportional (but not equal) to the subsurface contribution,  $c_S$ , which is always positive as well. Thus, the observations  $(c_{Ii}, c_{Ii}^\perp)$  must lie on the quarter of the unit circle within the positive quadrant.

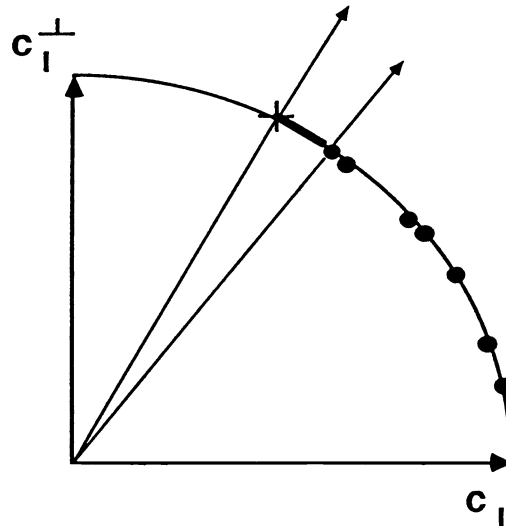


Fig. 3. Diagram of the  $(c_I, c_I^\perp)$  coordinates.

### C. Solution band

The observation of the surface reflectances are totally ordered along the quarter circle. As a contribution of the subsurface component increases, the observation point moves counterclockwise on the circle. The point for the pure subsurface reflectance function lies somewhere on the quarter circle. The only issue that remains, then, is to determine the direction of the vector  $S_S$  representing the subsurface reflectance  $S_S(\lambda)$ .

Lawton and Sylvestre<sup>5</sup> made the following observations. First, the requirement that both  $c_S$  and  $c_I$  be positive implies that the observations must fall within a cone defined by the direction of  $S_S$  and the horizontal axis  $c_I$ . It follows that directions that qualify as candidates for  $S_S$  must fall counterclockwise with respect to all of the data points. The data point closest to the  $c_I^\perp$ -axis ( $y$ -axis) defines this limit.

Second, the vector  $S_S$  representing the subsurface reflectance  $S_S(\lambda)$  must have all nonnegative elements. Not all vector directions satisfy this requirement. As we consider unit vectors in the clockwise direction from the  $c_I^\perp$ -axis, there will be a first direction in which all of the entries of the reflectance vectors are nonnegative. This direction is a second bound on the region of candidate directions for  $S_S$ . The true vector direction representing  $S_S$  must fall between this bound (marked by a "+" sign on the quarter circle in Figure 3) and the data point at the furthest counterclockwise direction. The set of permissible directions for describing the subsurface reflectance vector  $S_S$  is given by this band.

Both of these constraints may be stated using our notation. Suppose that we represent the vector direction of the subsurface reflectance as  $(r_1, r_2)$ . That is, the shape of the subsurface reflectance is represented in the form  $S_S(\lambda) = r_1 S_I(\lambda) + r_2 S_I^\perp(\lambda)$ . The requirement that the direction of  $S_S$  be counterclockwise to the last data point can be written as  $(r_2/r_1) \geq \max_{1 \leq i \leq m} (c_{Ii}^\perp/c_{Ii})$ , where the subscript  $i$  ranges over the  $m$  observations. The second requirement can be expressed as  $r_1 S_I(\lambda) + r_2 S_I^\perp(\lambda) \geq 0$  for all visible wavelengths  $\lambda_1, \lambda_2, \dots, \lambda_n$ . This can be written as  $(r_1/r_2) \geq \max_{1 \leq \lambda \leq n} (-s_{I\lambda}^\perp/s_{I\lambda})$ , where  $s_{I\lambda}$  and  $s_{I\lambda}^\perp$  are the elements of the vectors  $S_I$  and  $S_I^\perp$ , respectively. We can summarize the bounds on the direction of

the vector  $S_S$  in a single equation as

$$\max_{1 \leq i \leq m} \left( \frac{c_{Ii}^+}{c_{Ii}} \right) \leq \frac{r_2}{r_1} \leq \left[ \max_{1 \leq \lambda \leq n} \left( \frac{-s_{I\lambda}^+}{s_{I\lambda}} \right) \right]^{-1} \quad (12)$$

Any estimate of  $S_S(\lambda)$  with this bounded region satisfies all of the nonnegativity constraints and provides an equally satisfactory explanation of the data.

## 5 Experiments

We have carried out experiments to evaluate the present method of estimating the surface spectral reflectance function. The flow chart in Figure 4 describes the procedure. Two object surfaces are measured with different geometric conditions under a light source. First, the illuminant spectrum is estimated from the measured color signals. The observations of the surface spectral reflectances are then obtained by dividing the measured color signals by the estimated ambient light. The subsurface reflectance functions are estimated by the quarter circle analysis.

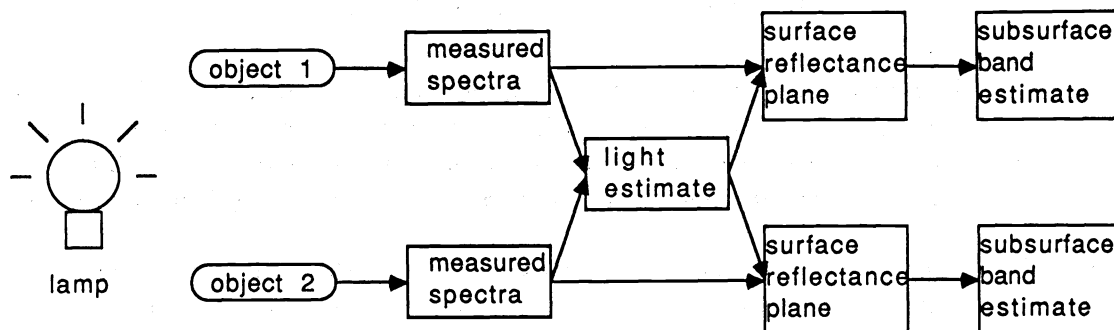


Fig. 4. Experimental procedure.

A red cup and a green ashtray were measured under a flood lamp for daylight photograph. The measured spectral data are shown in Figures 5 and 6 (see Ref.4). The estimate of the illuminant spectral power distribution is shown in a curve with filled squares in Figure 7. Figure 8 shows a set of the normalized curves of the surface spectral reflectances of the green ashtray  $S(\theta_i, \lambda)$  ( $i = 1, 2, \dots, 8$ ). Two principal components are extracted from the SVD, and the 2-by-2 transformation matrix is determined on the least-square fitting to the unit vector with entries of  $1/\sqrt{n}$ . Figure 9 shows the projection of the observed reflectances into the weighting coefficient coordinates  $(c_I, c_I^+)$ . Note that the observed points (black squares) fall on the unit quarter circle. The bounded region for  $S_S(\lambda)$  is given as the interval  $0.842 \leq r_2/r_1 \leq 1.293$  on the circle. A "+" sign indicates the upper limit, and corresponds to the limit of physically realizable reflectance curves. An estimate of the band of the subsurface reflectance function is shown in Figure 10, where a range of the subsurface estimates is given as the hatched band. The curve that has a point of tangency to the subsurface estimates is given as the hatched band. The curve that has a point of tangency to the wavelength axis is the theoretically limiting reflectance from nonnegativity. The other curve is the most extreme reflectance of real measurements. A width of the band is uncertainty of the estimates.

Furthermore we have applied our method to the reflectance estimation of objects measured under a fluorescent light source. A fluorescent lamp on the ceiling of an office emits such a spiky spectrum as shown in Figure 11. This time, two painted metals were measured with the ceiling lamp illumination. The surface reflectance of a metal painted yellow has been analyzed. We have an additional processing to treat the spikes. Figure 12 shows the final result of an estimated band of the subsurface reflectance functions of the painted metal.

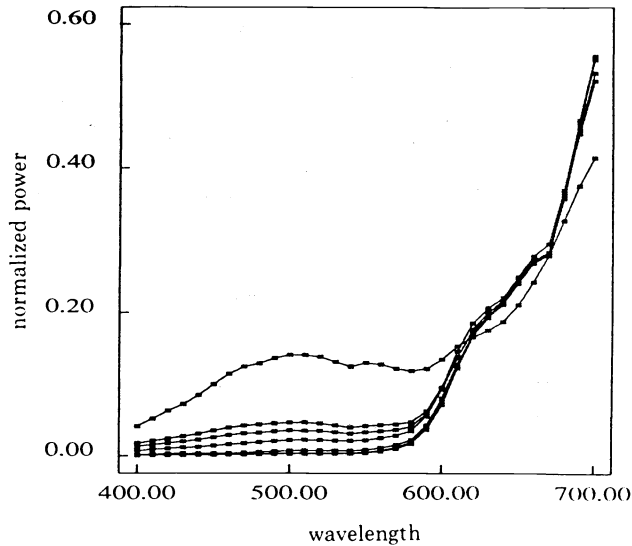


Fig. 5. Measured spectra of a red plastic cup.

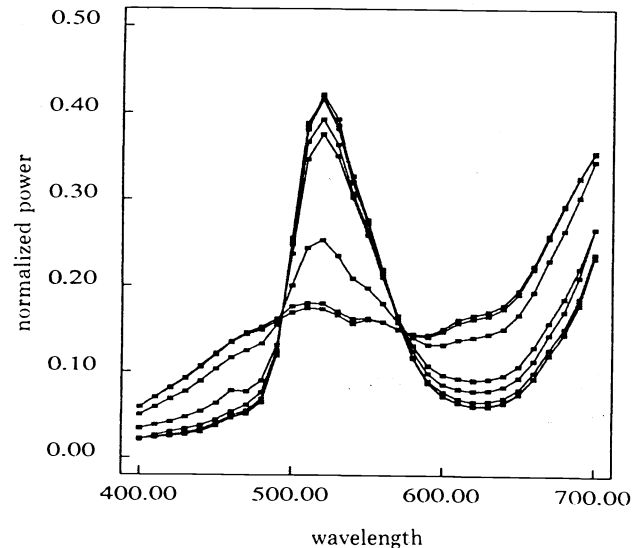


Fig. 6. Measured spectra of a green plastic ashtray.

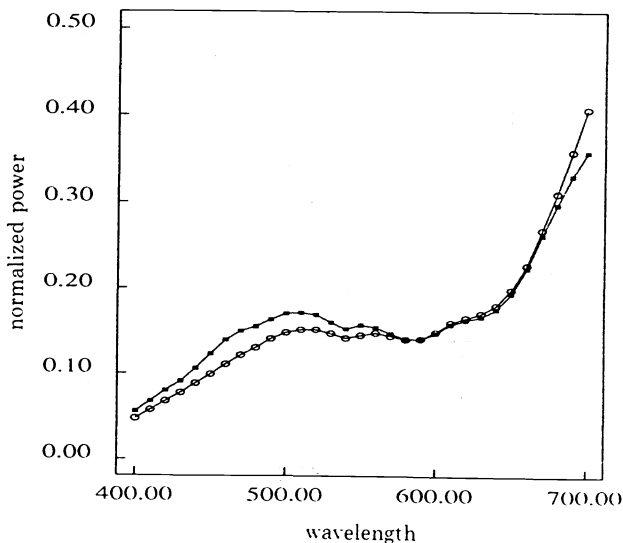


Fig. 7. Illuminant estimate of an flood lamp (filled squares).

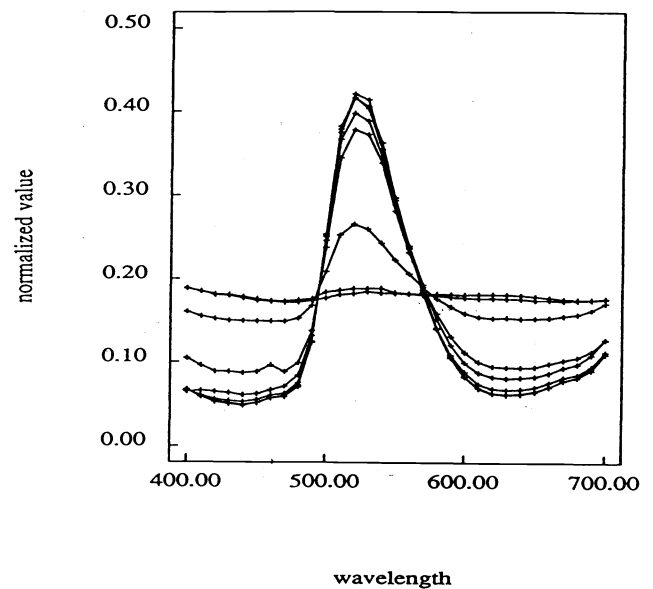


Fig. 8. Observed surface spectral reflectances of the green ashtray.

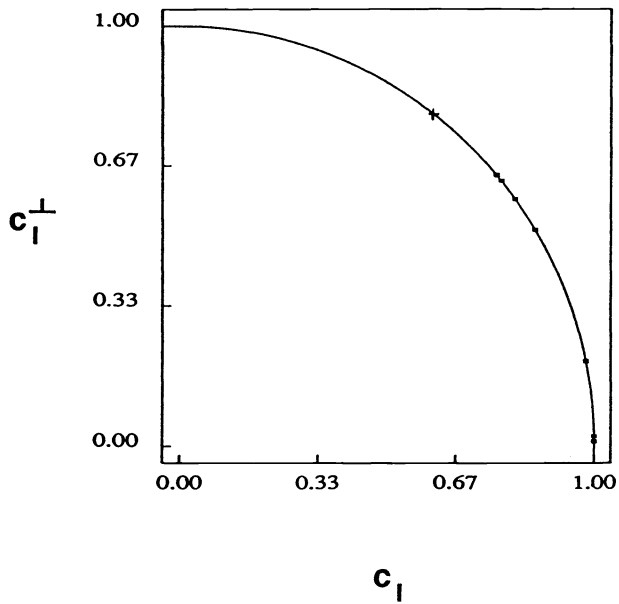


Fig. 9. Projection points of the surface reflectances.

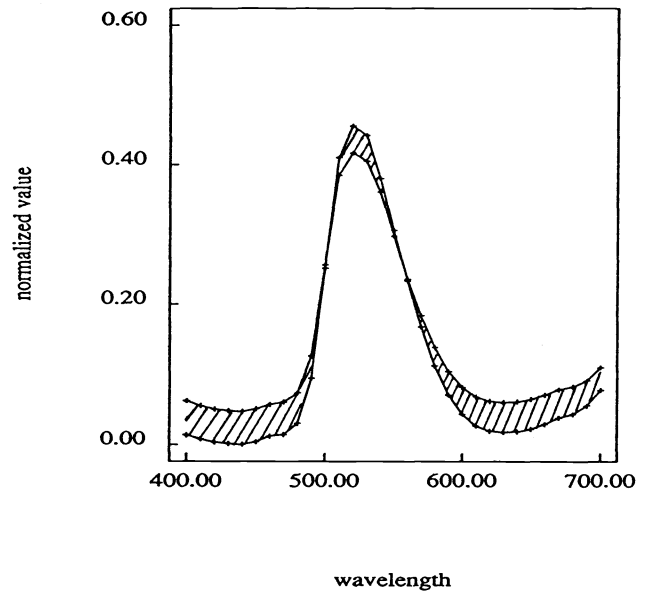


Fig. 10. Estimate of the band of subsurface reflectance functions of the green ashtray.

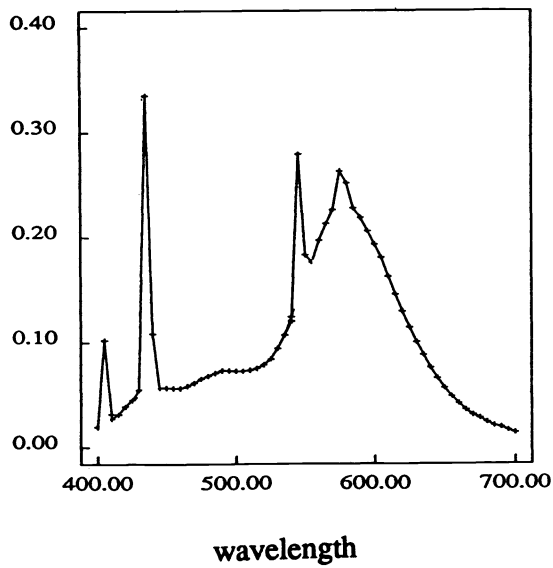


Fig. 11. Spectrum of a fluorescent lamp.

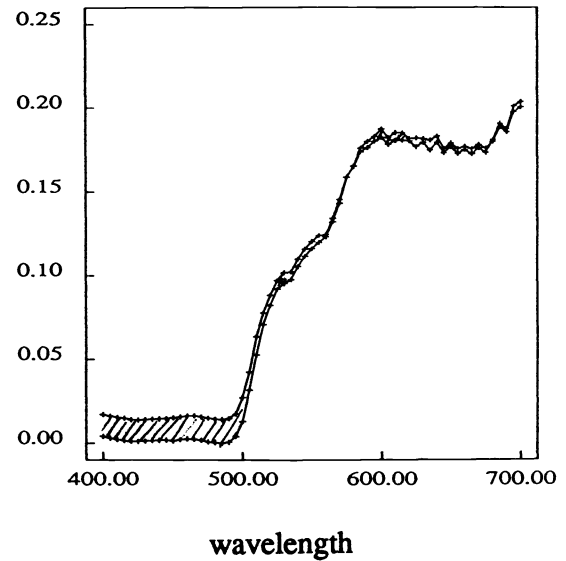


Fig. 12. Estimate of the band of subsurface reflectance of a yellow painted metal.

## 6 Conclusion

We have described a method for estimating the subsurface (diffuse) component of the surface reflectance function of inhomogeneous objects. First we use the property of constant specular reflection in the standard reflectance model to estimate an illuminant spectrum without using a reference white standard. Second we use several physical constraints on the reflectance functions to estimate the subsurface reflectance component. The method yields a band of the estimated spectral reflectance functions as possible solutions for the subsurface component. We consider that the method is applicable to the problem of perceiving objects in a natural scene.

## References

- [1] L. T. Maloney and B. Wandell, "Color constancy: a method for recovering surface spectral reflectance," *J. Opt. Soc. Am. A*, vol. 3, pp. 29-33, 1986.
- [2] R. L. Cook and K. E. Torrance, "A reflectance model for computer graphics," *Comput. Graph.* vol. 15, pp. 307-316, 1981.
- [3] G. J. Klinker, S. A. Shafer, and T. Kanade, "The measurement of highlights in color images," *International Journal of Computer Vision*, vol. 2, no. 1, pp. 7-32, 1988.
- [4] S. Tominaga and B. A. Wandell, "The standard surface reflectance model and illuminant estimation," *J. Opt. Soc. Am. A*, vol. 6, no. 4, pp. 576-584, 1989.
- [5] W. H. Lawton and E. A. Sylvestre, "Self modeling curve resolution," *Technometrics*, vol. 13, no. 3, pp. 617-633, 1971.